

# Feature Matching for Outer Orientation of Single Images Using 3-D Wireframe Controlpoints

Wolfgang Schickler

Institute of Photogrammetry  
University of Bonn, FRG

## Abstract

The paper presents an automatic model-based outer orientation (AMOR) of a single image using pattern recognition techniques. Models are 3-D wireframe models of buildings. The development of AMOR is part of an effort of the Survey Department Bonn, to automate the production of digital orthophoto maps. Extensive tests confirm the high reliability of the approach, and also the internal decisive measures for selfdiagnosis, and suggest the matching technique to be widely applicable.

**Key words :** Model-based object location, automatic outer orientation, 3-D matching, maximum likelihood estimators, selfdiagnosis.

## 1 Motivation

Digital orthophoto will soon replace their analog ancestor due to their versatility in use, their higher quality and certainly also lower costs. They will not only serve as a flexible basis for planning purposes, but also support quick map update.

Automatic orthophoto production needs several components to be available. A scanner and a plotter for digital input and output, a digital elevation model (DEM), information about the outer orientation and a powerful workstation. While concepts for differential rectification of digital images, programs for deriving DEM or possibly the DEM itself are available and integrated into systems, automatic procedures for determining the outer orientation are rare [e.g. MALMSTRÖM H. 86 ]

In case of a periodic update of orthophoto maps it is no longer necessary to perform an aerial triangulation each time, if there are automatically identifiable control points are available. Then the determination of the 6 orientation parameters may be achieved by individual spacial resections, which is unless costly. This was the motivation of the Survey Department Bonn to build up a control point database, consisting of more than 20 000 natural control points, mostly houses already more than 10 years ago. Within their up to now analog orthophoto production these control points were measured manually. In 1993 they will start to produce digital orthophotos. This change was the reason to develop a new concept concerning the automation of the whole production. The computer having access to the digital image data allows to replace the manual identification and measuring process by an automatic procedure allowing the setup of a production line fully independent of human observer. Whereas the rectification of the digital images causes no problem with respect full automation the identification of externally given objects, i. e. control points requires nothing more than a reliable image understanding procedure.

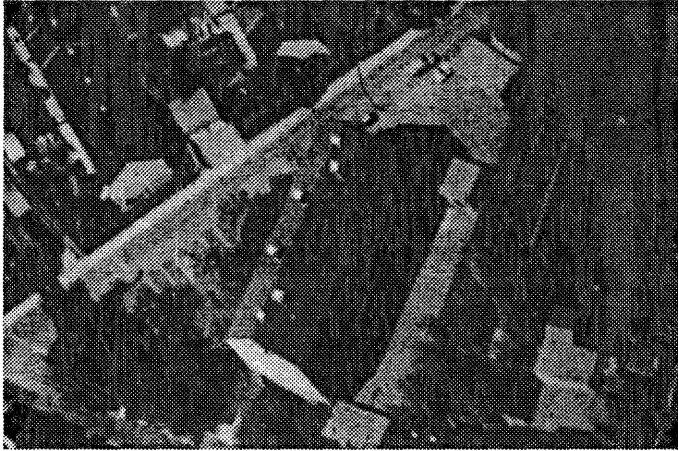
As pure correlation, thus low level matching, procedures are not feasible in this case, due to the three-dimensionality of the control points causing strong distortions, possibly occlusions, only an orientation procedure based on features is able to solve the matching task. More over, as the production has to be autonomous, the orientation procedure needs to contain a feature for selfdiagnosis, reliably predicting the success or failure of the procedure, as in (the unlikely) case of a failed orientation no rectification needs to be performed.

This paper describes the main features of the program AMOR for the automatic model-based orientation of aerial images. Though the actual procedure is optimized with respect to this task, the concept and most of the modules may be transferred to other applications.

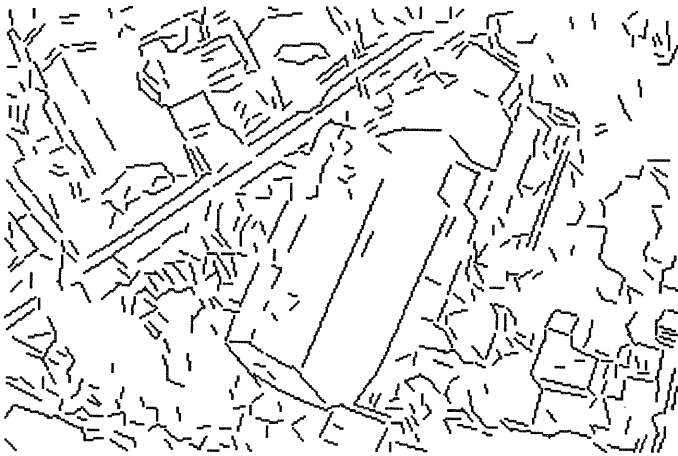
## 2 Overview

The orthophoto production of the Survey Department Nord Rhein Westfalen is based on images of approximate scale 1 : 12 000 which are digitized with a pixel size of  $25\mu m$ , a DEM and on a control point database. The control points, mostly roofs of houses, are given by orthographic sketches and 3D-coordinates of 2 distinct points. The sketches are used for the manual localisation of the control point buildings in the image. The density of the control points is high enough that 5 to 8 control points are available for outer orientation.

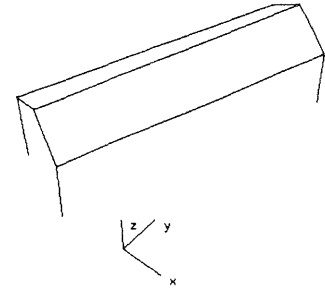
The possibility of using these 2-D sketches as models for object location based on uncertain models [FÖRSTNER W. 88 ; SESTER M. / FÖRSTNER W. 89] has been proved. The interpretation of the 2-D sketches lead to 3-D descriptions of the house roofs [SCHICKLER W. 89]. As the sketches have shown to be not fully in scale, the location process has been set up and realized in a way which took the uncertainty of the models into account, treating them as stochastic variables. Against previous assumptions, the sketches have shown to be not suitable for this purpose.



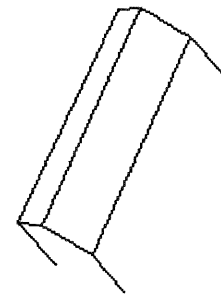
a. Subsection of an aerial image



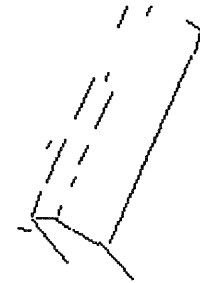
d. Extracted edges



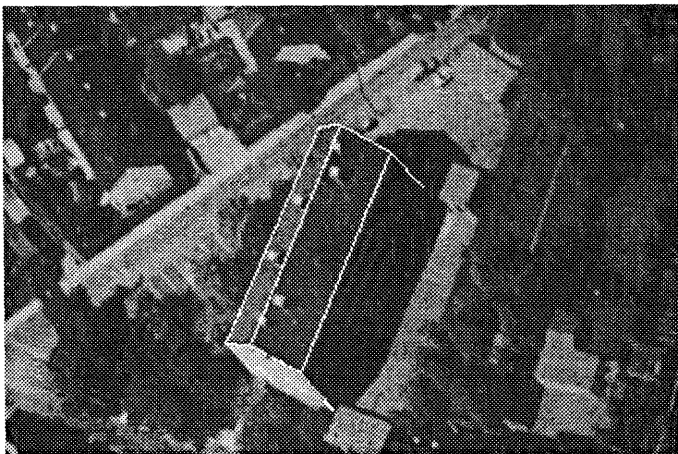
b. Perspectiv view of a 3-D control point model



c. Projected 2-D control point model



e. Preliminary set of matching candidates



g. Fited Model



f. Cleand set of matching candidates

Fig. 1 Example for control point location.

Therefore, now fixed 3-D wireframe models are used for the model-based control point location. The control point models are not any more treated as being stochastic. An approach for the automatic determination of the 3-D control point models is described in [BRAUN C. 92]. Available approximate orientation values enables us to reduce the searchspace of the matching process. The approximate geometry of the object up to a few degrees in the image, and its approximate location ( $\sim 50$  pixel) is known.

The whole automatic orientation procedure consists of following 6 steps (cf. Fig. 1). Step 1 to 3 are done separately for each controlpoint leading to a good approximate position of the controlpoints in the image. Step 4 to 6, the final evaluation of the orientation parameters, and the selfdiagnosis is done commonly for all controlpoints.

1. **Projection** of the 3-D control point model into the aerial image using the approximate orientation values. This projection leads to a 2-D wireframe control point model in the sensor system (cf. Fig. 1 b).
2. **Extraction** of straight line segments [SCHICKLER W.92] in a subsection of the digitized aerial image (cf. Fig. 1 d). The position of these subsections with respect to the whole image is derived from step 1. Its size depends on the precision of the approximate orientation values and the size of the control point building in the image. The inner orientation of the subsections is known, therefore the extracted line segments are determined in the image koordinate system. In case of color images the available color edge extraction [BRÜGELMANN R./FÖRSTNER W. 92] is applied.
3. **Probabilistic clustering** technique to determine approximate position of the controlpoint model in the subsection of the aerial image. This 2-D matching procedure leads to a preliminary set of matching candidates between image and model edges (cf. Fig. 1 e).
4. **Ransac** technique [CF. BOLLES R. C. / FISHLER M. A. 81] to find incorrectly located control point models and to predict a more likely set of matching candidates (not yet implemented).
5. **Robust estimation** to clean the whole set of preliminary correspondencies (cf. Fig. 1 f). This 3-D matching procedure is a final common fit of the 3-D controlpoint models to the image (cf. Fig. 1 g). It is a robust spacial resection using homologous straight line segments instead of homologous points leading to the orientation parameters of the aerial image.
6. **Selfdiagnosis** by analysing the final result with respect to precision and sensitivity considering the geometric configuration of the control points. This enables AMOR to decide whether the automatical determined orientation parameters are acceptable or have to be rejected.

### 3 The matching procedures

In many model-based object loaction concepts the matching problem is solved by a heuristic tree search procedure [c.f. GRIMSON W. / LOZANO-PÉREZ T. 87] The restrictions (cf. Section 2) allows to apply a special 2 step matching

procedure which is robust with respect to outliers and even in cases of weak information in the image able to locate the control point models correctly.

#### 3.1 Finding Candidates for Correspondencies via Clustering

The task of this procedure is to determine the approximate position of the projected model in the subsection of the image, to determine a set of matching candidates between image and model edges.

For each match of an image edge with a model edge the position of a reference point is calculated. This point can be chosen arbitrary but has to be fixed. As the length of the matched edges in general are not equal, a range of expected positions is added to the accumulator, taking the uncertainties of the extracted image edges into account. The final accumulator is a discretized version of the probability density function of the reference point, with a maximum for its most likely position. With this position one can derive a set of matching candidates between image and model edge. The propabilistic clustering has been described in [SESTER M. / FÖRSTNER W. 89]. It has be modified to treat all kinds of matches shown in Fig. 2.

If the given set of model features is unique, this 2-D matching technique is able to locate the model correctly even in cases where only a few (3 to 4 edges) corresponding image features are present. Unfortunately the uniqueness of the control point models is not always given due to weak model information. This may lead to partially wrong corespondencies or totally incorrect locations.

#### 3.2 Representation of the Straight Line Correspondencies

The clustering procedure results in a set of preliminary matches. Unfortunately the length of an image edge usually is not the same as the length of the corresponding model edge, due to occlusions, weak image information, shadows and so on. The final fitting of the models to the image is done by a robust spacial resection using homologous straight line segments, which has to cope with homologous lines also in case the length of model and image edge is not the same.

There are 7 possible cases of matching an image edge to a model edge:

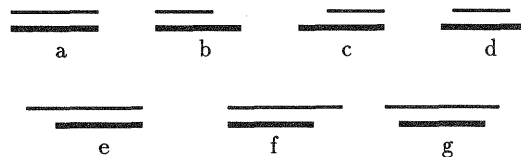


Fig. 2 Cases of matching an image edge (thin lines) to a model edge (thick lines)

The representation of these partial matches can not be done by individual point correspondencies, the image edges have to be treated as units holding the line information with possibly undefined start and (or) end point position.

This seperation of the line and point information can be done representing the image edge segments in the following manner:

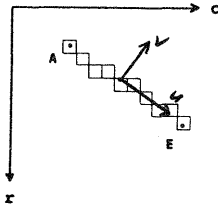


Fig. 3 Representation of a straight edge segment

Each edge segment with start point  $S$  and end point  $E$  is described in a local  $(u, v)$  coordinate system which lies near the principle axis of the edgels. In this local coordinate system the covariance matrix of the straight line parameters  $m$  and  $b$  of  $v = m \cdot u + b$  is diagonal and can be derived from the extraction process by error propagation. The  $v$ -coordinates of the end points of an edge element will be correlated due to the common factor  $m$  and will have following variances [FÖRSTNER W. 91]:

$$\begin{aligned} \sigma_{v_A}^2 &= \sigma_b^2 + u_A^2 \sigma_m^2 \\ \sigma_{v_E}^2 &= \sigma_b^2 + u_E^2 \sigma_m^2 \\ \sigma_{v_A v_E}^2 &= \sigma_b^2 + u_A u_E \sigma_m^2 \end{aligned} \quad (1)$$

The  $u$ -coordinates of the two end points can be treated as uncorrelated because the accuracy in  $u$ -direction is mainly influenced by roundig errors. Therefore the uncertainty of the the  $u$ -coorinates could be represented by having the variance  $\approx 1/12[\text{pixel}]$ , or any other reasonable variance taking the edge extraction process into account.

Thus the covariance matrix and especially the weight matrix of an edge segment in the local coordinate system  $(u, v)$  will have the following structure:

$$\Sigma^{(u,v)} = \begin{pmatrix} \sigma_{v_A}^2 & 0 & 0 & 0 \\ 0 & \sigma_{v_A}^2 & 0 & \sigma_{v_A v_E} \\ 0 & 0 & \sigma_{u_E}^2 & 0 \\ 0 & \sigma_{v_A v_E} & 0 & \sigma_{v_E}^2 \end{pmatrix} \quad (2)$$

$$\mathbf{W}^{(u,v)} = \begin{pmatrix} w_{u_A}^2 & 0 & 0 & 0 \\ 0 & w_{v_A}^2 & 0 & w_{v_A v_E} \\ 0 & 0 & w_{u_E}^2 & 0 \\ 0 & w_{v_A v_E} & 0 & w_{v_E}^2 \end{pmatrix} \quad (3)$$

Transforming the edge segment back into the image coordinate system  $(r, c)$  yields the covariance and weighting matrix

$$\Sigma^{(r,c)} = \mathbf{R} \cdot \Sigma^{(u,v)} \cdot \mathbf{R}^T \quad (4)$$

$$\mathbf{W}^{(r,c)} = \mathbf{R} \cdot \mathbf{W}^{(u,v)} \cdot \mathbf{R}^T \quad (5)$$

with the rotation matrix

$$\mathbf{R} = \begin{pmatrix} \mathbf{R}_\phi & 0 \\ 0 & \mathbf{R}_\phi \end{pmatrix} \quad (6)$$

The rotation matrix  $\mathbf{R}$  is only depending on the individual direction  $\phi$  of the edge segment in the image coordinate system.

This kind of representation of the uncertainty of an image edge segment does not depend on whether the start or end point are longitudinally linked to the model edge. The edge segments are treated as units holding the line information with possibly undefined start and (or) end point position.

This enables handling of different cases of matching an image edge to a model edge shown in Fig. 2.

Homologous lines having different length now can be represented by treating their end point pairs like normal points, but with a joint covariance or weight matrix resp. . The spacial resection is based on these properly weighted end point pairs. One simply had to set the weights (cf. equation ??) seperately for the start and end point correspondencies. For example case d in Fig. 2 could be represented by setting  $w_{u_A}$  and  $w_{u_E}$  to zero.

This favourable property will be used in the robust estimation (cf. section 3.3). At the beginnig all weights are set corresponding to case a) (hypothese : complet match). The weights will be iteratively modified in the robust estimation realizing the partial matches.

### 3.3 Determining the Final Position via Robust Estimation

The clustering procedure is done seperately for each control point model in the aerial image leading to a list of possibly corresponding straight line segments for the whole image, i.e. for all control points. In addition to the partial matches mentioned in section 3.2 (wrong start and end point correspondencies), this list contains two kinds of gross errors. The first one is due to the design of the conservative test in that matching procedure which results in wrong edge correspondencies though the control point model was located correctly. The second and more severe error is a partially or completely incorrect location due to a weak model or weak image information. Both error sources lead to wrong correspondencies between image and model edge.

To clean these inconsistencies a robust estimation [HAMPEL 86 / HUBER P. J. 81] is applied for the final common fit of the control point models and the evaluation of the orientation parameters. Wrong correspondencies are interpreted as outliers or as observations with large deviations from the mean value.

The used robust estimation, which is a ML-type estimator, is able to cope with outliers up to 30%. In comparison with least square (LS) technique which minimizes

$$\Omega = \Sigma e_i^2 w_i \quad (7)$$

with the weights  $w_i = \frac{1}{\sigma_{x_i}^2}$

one has to minimize a less increasing function  $\tau$

$$\Omega = \Sigma \tau(e_i \sqrt{w_i}) \quad (8)$$

of the normalized residuals leading to the normal equations

$$\Sigma \tau'(e_i \sqrt{w_i}) a_{ij} w_i = 0 \quad (9)$$

with  $\tau'(x)$  being the derivative of the minimum function  $\tau(x)$ .

There are two ways to modify a standart LS technique to solve these systems (eq. 8 and 9). One could use adapted weights or adapted residuals, both leading to an iteaive LS procedure. Here the method of modified weights is used because this simplifies the handling of the partial matches mentioned in section 3.2. Using a **weight function**  $f(t) = \tau(t)/t$  and the following iteration scheme for calculating the weights for the  $k$ -th iteration

$$w_i^k = w_i^0 \cdot f(t_i^{k-1}) \quad (10)$$

leads to an iterative LS procedure weighting down those observations with large test statistics  $t$ .

As weight function a weighted combination of the following two functions are used

$$f_1(t) = \frac{1}{\sqrt{1 + (t/c)^2}} \quad \text{and} \quad f_2(t) = \exp\{-0.5(t/c)^2\} \quad (11)$$

with the critical value  $c = 3$ .

The first function guarantees a global convergency. The second one cancels the effect of large outliers onto the result [cf. HAMPEL 86 / FÖRSTNER W. 89]. The influence of the second function at the first iteration is zero and continuously increasing with each iteration. Therefore the inconsistencies depending on the problem of partial matches are cleaned in the first few iterations while the effect of the wrong correspondences between image edge and model edge onto the result is increasingly reduced with each iteration.

The observation equation for the LS-fitting of the 3-D control point models into the image are given by the well known equations of a spatial resection here applied to homologous straight line segments. For each homologous line a set of following 4 equations is added to the normal equations resulting from equating the start point and end point of an image edge  $p^i$  to the start and end point of the model edge  $p^m$  using the projective equations.

$$\begin{pmatrix} p_s \\ p_e \end{pmatrix}^i + \begin{pmatrix} e_s \\ e_e \end{pmatrix} = \begin{pmatrix} p_s \\ p_e \end{pmatrix}^m (y) \quad (12)$$

The weight matrix is given by eq. 3.

The start and end point for each homologous line are treated separately to allow all the partial matches shown in Fig. 2, especially when calculating the weights using eq. 3 respectively eq 5. The measurement checking the start point-, the end point- and line-hypotheses are test statistics with respect to the local coordinate system  $(u, v)$ . To calculate these statistics the residual vectors  $e_s$ ,  $e_e$  and the covariance matrix of the residuals has to be transformed into the local coordinate system using the same rotation matrix  $R_\phi$  shown in eq. 6. Thus the test statistics  $t$  are calculated as

$$\begin{aligned} t_s &= e_{u_s} / \sigma_{u_s} \\ t_e &= e_{u_e} / \sigma_{u_e} \\ t_l^2 &= (e_{v_s} e_{v_e}) \Sigma_{vv}^{-1} \begin{pmatrix} e_{v_s} \\ e_{v_e} \end{pmatrix} / 2 \end{aligned} \quad (13)$$

The residuals in the local  $(u, v)$  system are analogous to longitudinal and lateral error of the fit of image and model edge. Thus these test statistics are the proper measurements for checking the start point-, the end point- and line-hypotheses. The test statistic are normally and (square root) Fisher distributed. We have

$$t_s \sim N(0, 1), \quad t_e \sim N(0, 1), \quad t_l \sim \sqrt{F_{2, \infty}}. \quad (14)$$

The test for the point or line-hypotheses consists of comparing the test statistics with critical value e.g.  $c = 3$ . If the test statistics exceeds the critical value, for numerical reasons

the weight of the observation is set to zero so having no influence on the result. Otherwise it is used to calculate the respective weights in the manner previously described.

The test statistics  $t_s$  and  $t_e$  are used to weight down the wrong the start and (or) end point correspondencies. From the statistical point of view this means: Keep the line information while rejecting the hypothesis that the start and (or) end point of the image edge matches the start and (or) end point of the model edge.

The test statistic  $t_l$ , which measures the lateral error is used to weight down or eliminate wrong edge correspondencies.

Thus after 6 to 8 iterations the above described outliers are eliminated or weighted down so heavily that their influence onto the result can be neglected.

## 4 Selfdiagnosis

It is important for each automatic system that it is able to make a selfdecision for the acceptance of the result. The orientation procedure presented in this paper, is part of an automatic process which is planned to run in night-time or on weekends without any human manipulation. Therefore the system must be able to decide whether the determined orientation parameters are correct or better had to be rejected. Thus an objective quality control measure is necessary. Gross errors can hide behind small residuals or excellent fitting of data and model, therefore they do not necessarily produce large variances in the estimated parameters. Therefore a additional sensitivity analysis for selfdiagnosis is used.

The concept of sensitivity analysis developed by Baarda [BAARDA W. 67, 68] is based on the measures for the internal and external reliability. The elementary theory has been expanded and specified for our purpose [cf. FÖRSTNER W. 83, 92]. The sensitivity analysis is used to investigate the influence of a single control point model onto the estimated orientation parameters, taking the geometry of the design (control point arrangement) into account. A single control point model is represented by several image to model edge matches. Therefore the sensitivity analysis is applied to groups of observations, namely all the edges belonging to one control point model.

The following measures, calculated for each control point model in the aerial image, are used for evaluating the quality of the orientation:

The Fisher test statistic

$$T_i^2 = \frac{e_i^T \Sigma_{e_i e_i}^{-1} e_i}{r_i \hat{\sigma}_0^{(i)2}} \quad (15)$$

depends on the geometry of the design and the size of an undetected gross error in the observation group  $x_i$ . This test statistic is Fisher distributed. A gross error in the observation group  $x_i$  could be detected with a significance level  $\alpha$  by checking

$$T_i^2 > F(\alpha, n_i, n - n_i) \quad (16)$$

with

$$\begin{aligned} n_i &= (\text{Number of image edges from model } i) \cdot 4 \\ n - n_i &= (\text{Number of the remaining image edges}) \cdot 4 \\ \alpha &= \text{significance level e.g. 95\%} \end{aligned}$$

**The Influence factor**

$$\mu_i^2 = \lambda_{max}^2 [(\Sigma_{yy}^i - \Sigma_{yy}) \Sigma_{yy}^{-1}] \quad (17)$$

measures the maximum increase  $\Sigma_{yy}^{(i)} - \Sigma_{yy}$  of the uncertainty  $\Sigma_{\hat{y}\hat{y}}$  of the estimated parameters  $\hat{y}$ , if the observations group  $x_i$  is omitted with respect to  $\Sigma_{\hat{y}\hat{y}}$ . It reduces to  $\mu_i^2 = (1 - r_i)/r_i$  for single observations [cf. BAARDA W. 87].

**The empirical sensitivity**

$$\bar{\delta}_i = T_i \cdot \mu_i \quad (18)$$

measures the maximum influence of the observations group  $x_i$  onto the estimated parameters. If this group is omitted an arbitrary function  $f = a^T \cdot y$  of the estimated parameters  $y$  with variance  $\sigma_f^2 = a^T \Sigma_{yy} a$  does not change more than

$$\nabla_i f \leq \bar{\delta}_i \cdot \sigma_f \quad (19)$$

A great value indicates the observation group  $x_i$  to be necessary, namely the control point model  $i$  to improve the result. In case the value is small the result is determined reliably as the control point is checked by the others and the control point model only slightly influences the result.

**The theoretical sensitivity**

$$\bar{\delta}_{i0} = \delta_0 \cdot \mu_i \quad (20)$$

(external reliability according to BAARDA) gives the maximum influence of undetected errors in observation group  $i$  onto the estimated parameters. The influence of an undetected error in the observation group  $i$  is bounded by

$$\nabla_{0i} f \leq \bar{\delta}_{0i} \cdot \sigma_f \quad (21)$$

with  $\delta_0$  depending on the significance level and the required power of the test, we use  $\delta_0 = 4.13$ .

Small values indicate that an error not detectable by the robust estimation has an influence onto the result that can be neglected. Large values indicate a unacceptable control point arrangement.

**5 Conclusions**

An automatic outer orientation procedure of aerial images based on 3-D wireframe models of natural control points was presented. The matching procedures for finding correspondencies between image and model features, namely straight line segments, have shown to be robust, with respect to wrong or missing correspondencies. The examples demonstrates the feasibility of object location with this approach even in case of weak image information, being the normal case in natural scenes especially aerial images.

The sensitivity analysis applied to groups of observations here used as a means for selfdiagnosis has shown as a powerful tool for the automated system to be used in practice. The program system AMOR has been tested on 32 aerial images. In 5 cases the sensitivity analysis correctly supposed a weakly determined configuration, though the orientation parameters were correct. In 11 cases the clustering has made a wrong correspondence which has correctly been detected by the robust estimation, therefore the orientation parameters has been correct. In the other cases all the control points

has been correctly located. The program system AMOR will be implemented this year into the automatic orthophoto production system at the Survey Department Bonn.

Though the actual procedure is optimized with respect to the task of automatic outer orientation of aerial images, the concept and most of the modules, especially the matching procedures, may be transferred to other applications. In section 6 an example is presented using the presented matching procedures for semiautomatic mapping.

**6 Examples**

**Example 1 :**

Detecting bad geometric control point configurations via Selfdiagnosis.

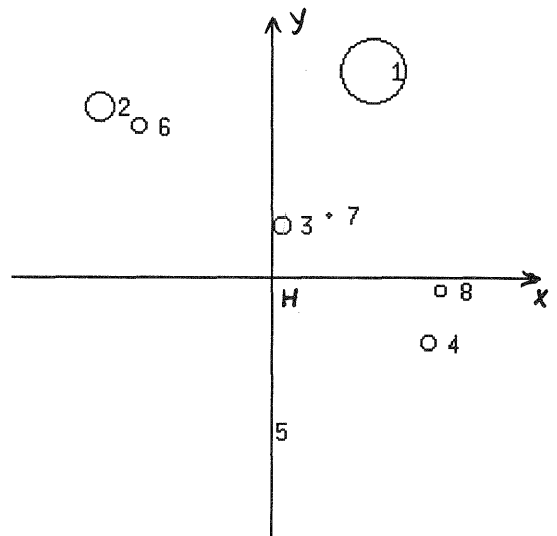


Fig. 4 Configuration of 8 control points in an aerial image

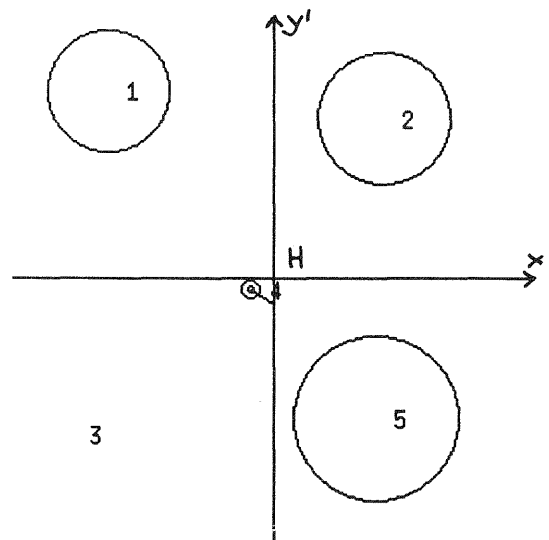


Fig. 5 Configuration of 5 control points in an aerial image

Fig. 4 demonstrates the configuration of 8 control points. The circles mark the location of the control points with respect to the image coordinate system  $(x,y)$ . The radius of the circles depends on the empirical sensitivity  $\delta_{oi}$ . Point 5, falsely located by the clustering procedure due to weak model information, has been correctly eliminated by the robust estimation. The other points except point 1 ly near a straight line. Therefore point 1 is necessary to stabilize this configuration. This is automatically found by the sensitivity analysis.

Fig. 5 shows a configuration of 5 control points. Point 3, falsely located by the clustering procedure due to weak image information, has been correctly eliminated by the robust estimation. The other points ly in a bad geometric configuration. The point 4 near to the principle point, causes any 3 of the 4 points to make the projection centre ly on the critical cylinder. This is automatically found by the sensitivity analysis.

**Example 2:**

An other application of the matching procedures:

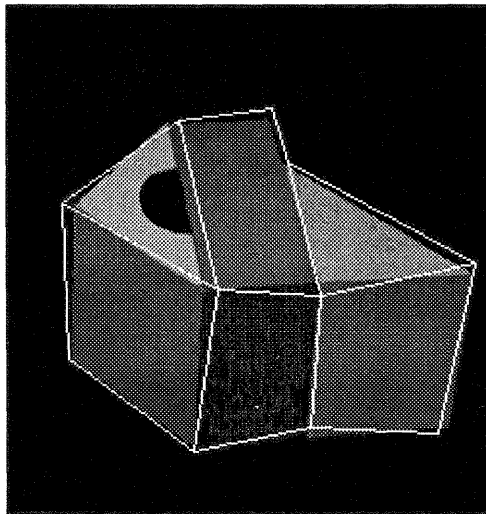


Fig. 6 Roughly and manually digitized object

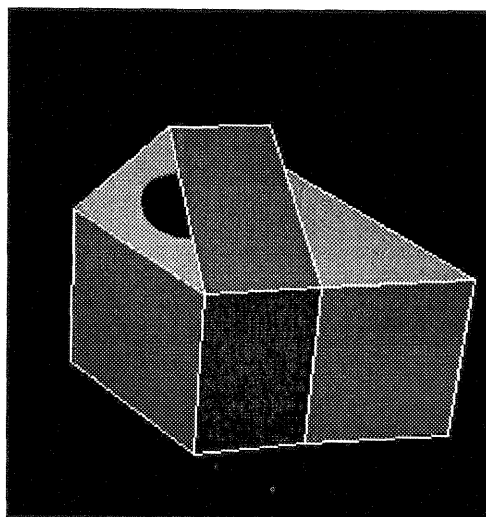


Fig. 7 Result of the matching procedure

This is an example for using the matching procedure for semi-automatically mapping. The object being of interest can be quickly and roughly digitized using a mouse cursor (cf. Fig. 6) which than is exactly fitted to the image (Fig. 7) using the matching procedure described in this paper. The observation equation for this approach are given by simply equating the end points of the extracted edges to the corresponding roughly digitized model edge according to eq. 12, but without using any projective function. The model points are treated as estimates. As the straight line extraction could run while the operator is digitizing, the fitting of the model to the image for this example takes less than 1 second on a SUN Sparc 2.

**Example 3 :**

Result of a control point location

Image scale: 1 : 12 000, Pixelsize:  $25 \mu m = 30 cm$ .

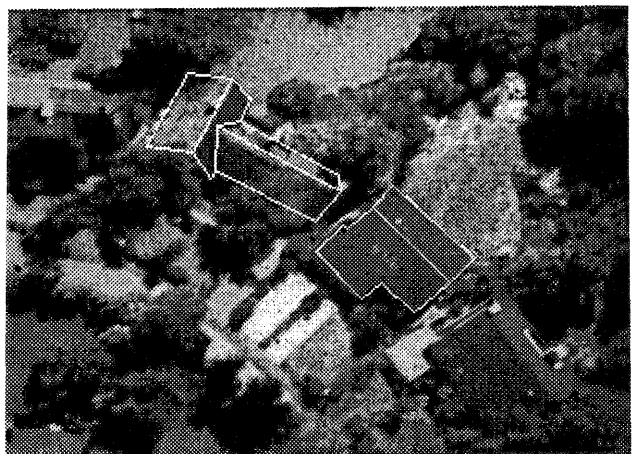


Fig. 8 Result of the control point location

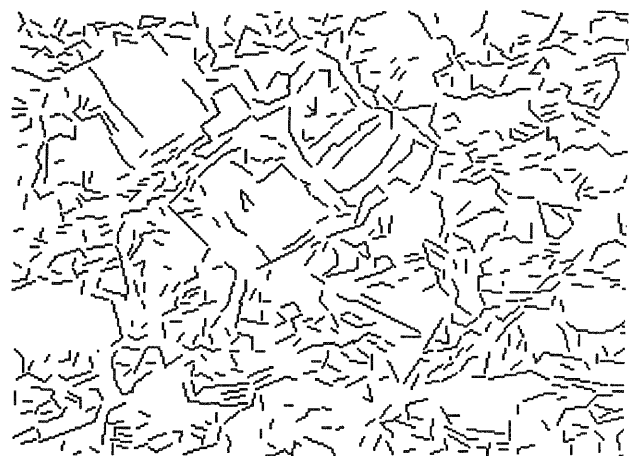


Fig. 9 Extracted straight line segments



Fig. 10 Cleaned set of matching candidates

#### Example 4 :

Result of a control point location

Image scale: 1 : 12 000, Pixelsize: 25  $\mu\text{m}$  = 30 cm.

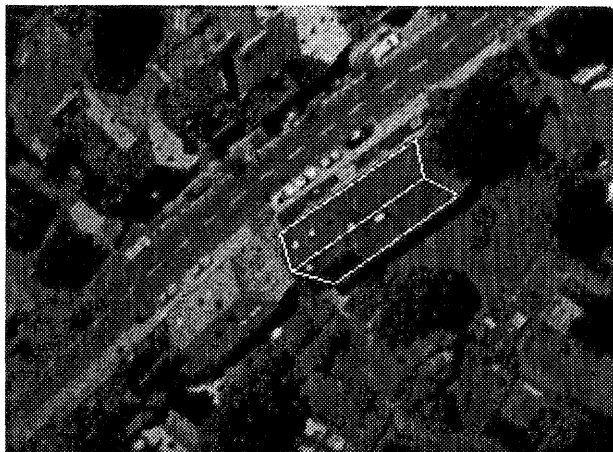


Fig. 11 Result of the control point location

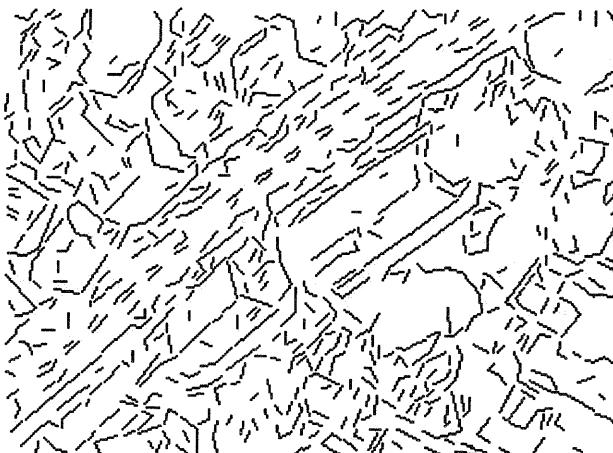


Fig. 12 Extracted straight line segments



Fig. 13 Cleaned set of matching candidates

## References

- [BAARDA W. 67] Statistical Concepts in Geodesy, Netherlands Geod. Commission New Series, Vol. 2, No. 4 Delft, 1967
- [BAARDA W. 68] A Testing Procedure for Use in Geodetic Networks, Netherlands Geod. Commission New Series, Vol. 2, No. 5 Delft, 1968

- [BOLLES R. C., FISHLER M. A. 81] Random Sample Consensus: A Paradigm for Model Fitting with Applications to Image Analysis and Automated Cartography, *Comm. of ACM*, Vol. 24, No. 6, 1981 pp 381 - 395
- [BRAUN C. 92] Interpreting Single Image of Polyhedra, *ISPRS 92*, Comm. III, Washington, 1992
- [BRÜGELMANN R., FÖRSTNER W. 92] Noise Estimation for Color Edge Extraction, in *Förstner/Ruwiedel 1992: Robust Computer Vision*, Wichmann, Karlsruhe, 1992, pp 90 - 106
- [FÖRSTNER W. 83] Reliability and Discernability of Extended Gauss-Markov Models, *Deutsche Geod. Kommission A98*, München, 1983, pp 79 - 103
- [FÖRSTNER W. 87] Reliability Analysis of Parameter Estimation in Linear Models with Applications to Mensuration Problems in Computer Vision, *CVGIP 40*, 1987, pp 87 - 104
- [FÖRSTNER W. 88] Model-Based Detection and Location of Houses as Topographic Control Points in Digital Images, *ISPRS*, Vol. 27, Part B11, 1988, pp III505 - III517
- [FÖRSTNER W. 89] Robust Methods for Computer Vision, Tutorial, *IEEE Computer Society Conference on Computer Vision and Pattern Recognition*, San Diego 1989
- [FÖRSTNER W. 91] Statistische Verfahren für die automatische Bildanalyse und ihre Bewertung bei der Objekterkennung und -vermessung, *Deutsche Geodätische Kommission, Reihe C, Heft Nr. 370*, München, 1991, pp 54 - 61
- [FÖRSTNER W. 92] Quality of Vision Algorithms, Tutorial, Bonn, *Institut für Photogrammetrie*, 1992, pp 30 - 40
- [GRIMSON W., LOZANO-PÉREZ T. 87] Localizing Overlapping Parts by Searching the Interpretation Tree, *IEEE T-PAMI 9*, 1987, pp 469 - 482
- [HAMPEL 86] Robust statistics, The Approach Based on Influence Functions, Wiley, NY, 1986
- [HUBER P. J. 81] Robust Statistics, Wiley, NY, 1981
- [MALMSTRÖM H. 86] Measuring Ground Control Points for Satellite Image Rectification, *Proc. Photogrammetric Week 40*, Vol. 11, 1986, pp 127 - 135
- [SCHICKLER W. 89] Interpretation von Hausskizzen, Diplomarbeit, Universität Stuttgart, 1989
- [SCHICKLER W. 92] Bildkanten für Meßaufgaben in der digitalen Photogrammetrie, *Zeitschrift für Photogrammetrie und Fernerkundung 3/92*, Wichmann, Karlsruhe, 1992
- [SESTERS M., FÖRSTNER W. 89] Object Location Based on Uncertain Models, *Informatik Fachberichte*, Springer, 1989, pp 457 - 464